Placement of Virtual Synchronous Generator Controlled Electric Storage combined with Renewable Generation

Junru Chen, Muyang Liu, Federico Milano and Terence O'Donnell
University College Dublin
School of Electrical and Electronics Engineering
Dublin, Ireland
{junru.chen.1; muyang.liu}@ucdconnect.ie, {federico.milano; terence.odonnell}@ucd.ie

***Abstract*— The virtual synchronous generator (VSG) control of power converters has been proposed to improve the system inertia. The commonly used VSG requires an energy storage (ESS) to provide the emulated inertia power and the frequency droop power. The placement of the ESS can be either in the DC port of the power electronics generation or co-located with the power electronics generation on the AC side. In the former case, the VSG control makes the total generator behave like a synchronous generator, while in the latter one, the VSG control only regulates the ESS in response to the grid frequency. The different placement of the ESS gives rise to different performance. This paper analyzes this performance firstly by means of simple transfer function analysis and secondly by comparing their effects on the grid frequency at the system level in the IEEE 39 bus test system. The results show that the placement of the ESS has no impact on the system transient stability while it has a significant impact on the frequency dynamics especially in the low inertia situation.**

***Index Terms*—Storage, Virtual Synchronous Generator, power system simulation, higher wind penetration**

I. INTRODUCTION

The movement from the synchronous generation to the power electronics generation, such as wind farm and solar plant, reduces the inertia of the system and further leads to the transient instability. This action requires that the storage not only compensates power to the steady state frequency deviation but also needs to respond to the rate of change of frequency (ROCOF), thus emulating the behavior of inertia. In 2007, Beck and Hesse proposed the virtual synchronous generator (VSG) concept, which controls the interfaced power converter to mimic the synchronous generator (SG) by means of the swing equation emulation with virtual inertia [1]. The electric storage (ESS) in this method is controlled to provide the emulated inertia power during transients to support the grid frequency.

Different implementation approaches on the virtual inertia emulation have been well researched [2-8]. The outer control loop of the converter is either voltage regulation or power regulation [9,10], thus, the VSG control can be implemented for either approach. In the outer power regulation type, the power reference is computed by the swing equation with gains for the frequency deviation and ROCOF, while the grid frequency is detected by the phase locked loop (PLL). Although this method is easily achieved with a small modification in the current droop-controlled ESS, its terminal voltage is only indirectly controlled in order to send the reference power into the grid. However, if the power system is to be solely supplied by power electronics generation, the converter must move from the grid-feeding to the grid-forming control in order to establish the voltage in the grid. Based on this point, the voltage-controlled VSG was proposed [5-8]. In this type, the swing equation is used to achieve the synchronization and phase determination, while the reactive power to voltage regulation is used to determine the voltage amplitude. This type of the VSG forms the voltage and frequency in the same manner as the SG with the inclusion of primary controls, i.e. automatic voltage regulation (AVR) and turbine governor (TG).

Ideally, in the voltage type of the VSG, the ESS should directly connect into the DC port of the renewable energy source, and the renewable and ESS generation share the same converter interfacing to the grid [11-13]. The implementation of the VSG control into this converter can make the whole renewable energy system behave like the synchronous generation. However, typically the conventional grid converter of the renewable generation works with an outer power regulation or as grid feeding [10]. Moreover, the connection of the ESS in the DC port necessitates an increase in the grid-converter capacity which for existing wind plant would require replacement of the converter, which is costly. A compromise approach is to install the VSG-controlled ESS co-located with the existing renewable energy sources. These two

This work is funded by the Science Foundation Ireland (SFI) under Grant Number SFI/15/SPP/E3125 and SFI/15/IA/3074.

different structures will have different performance. The objective of this work is to investigate the performance of both approaches. To do this a device level performance comparison for connection to an infinite bus is performed through full switching model simulations. Next a simple transfer function analysis is presented to analyze the dynamics when connected to a power system represented as a single equivalent synchronous generator. Finally, using a differential-algebraic models of the VSG system [5-8], which has previously been validated using the hardware-in-the-loop [8], the performance of both approaches is compared in terms of resulting system level frequency dynamics when inserted in the IEEE 39 bus test system. Several system level scenarios with different penetration levels of wind generation are presented. The contribution of this paper is to compare the effects of the ESS placement in combination with renewable generation especially as the power system moves towards being converter dominated.

The paper is organized as following: Section II briefly reviews the VSG control. Section III introduces the different placement of the ESS in the renewable generations. Section IV uses transfer function analyzing the effect of the ESS placement on the grid frequency. Section V compares the effect of the different placement of the ESS on the stability in the IEEE 39 bus system.

II. VIRTUAL SYNCHRONOUS GENERATOR

The VSG control is applied as the outer loop of the conventional voltage source converter control, which acts as the reference provider. The VSG control includes three parts, the active power regulation, voltage regulation and virtual impedance. The VSG control scheme is given in Fig. 1. The active power regulation is used to determine the emf phase δ by the application of the swing equation (1) with virtual inertia M and droop/damping D to achieve self-synchronization, where ω^* is the reference frequency, ω_{base} is the base frequency, ω_{VSG} is the VSG frequency, ω_{grid} is the grid frequency, P^* is the feed-forward renewable generation power, and P is the VSG output power. If the VSG is solely implemented into the ESS system, then P^* is set to 0. The voltage regulation (2) is similar to the AVR, which determines the emf amplitude E and tries to maintain the grid voltage V_g at rated V^*. The virtual impedance $r_v + jx_v$ is used to mimic the SG stator impedance and appears as connecting to the grid impedance in series, which could help modify the transmission impedance and decouple the active and reactive power. The reference voltage v_o^* is the emf minus the voltage dropped on the virtual impedance as (5), where i_d/i_q is the current. The converter outer voltage control, inner current control and LC filter parts are modelled as (4), (5) and (6) respectively, where K_{pv}/K_{iv} is the voltage controller PI gain, K_{pc}/K_{ic} is the current controller PI gain, and the electric components and elements are notated in Fig. 1. The power P/Q transmitting from the VSG output to the grid through the line $r_g + jx_g$ with dynamics (7) is computed in (8) and feeds back to the swing equation in (1). Equation (1~8) is the differential-algebraic model of the VSG system. The more detailed modelling description is given in [8].

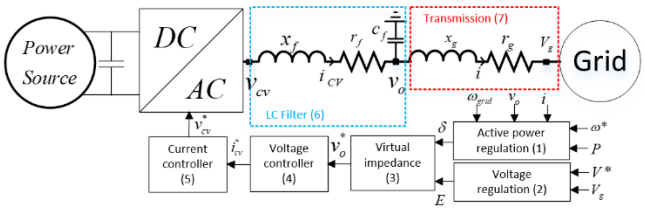

Fig 1. VSG controlled WG.

$$\left.\begin{aligned} M\frac{d\,\Delta\omega_{VSG}}{dt} &= P^* + D(\omega^* - \omega_{VSG}) - P \\ \Delta\omega_{VSG} &= \omega_{VSG} - \omega_{grid} \\ \frac{d\delta}{dt} &= \Delta\omega_{VSG}\,\omega_{base} \end{aligned}\right\} \quad (1)$$

$$E = V^* + K_v\left(V^* - V_g\right) \quad (2)$$

$$\left.\begin{aligned} v_{od}^* &= E + \omega_{VSG}x_v i_q - r_v\, i_d \\ v_{oq}^* &= -r_v i_q - \omega_{VSG}x_v i_d \end{aligned}\right\} \quad (3)$$

$$\left.\begin{aligned} i_{cvd}^* &= K_{pv}(v_{od}^* - v_{od}) + K_{iv}\varepsilon_d - \omega_{VSG}c_f v_{oq} \\ i_{cvq}^* &= K_{pv}\left(v_{oq}^* - v_{oq}\right) + K_{iv}\varepsilon_q + \omega_{VSG}c_f v_{od} \\ \dot{\varepsilon_d} &= v_{od}^* - v_{od} \\ \dot{\varepsilon_q} &= v_{oq}^* - v_{oq} \end{aligned}\right\} \quad (4)$$

$$\left.\begin{aligned} v_{cvd}^* &= K_{pc}(i_{cvd}^* - i_{cvd}) + K_{ic}\gamma_d - \omega_{VSG}x_f i_{cvq} \\ v_{cvq}^* &= K_{pc}\left(i_{cvq}^* - i_{cvq}\right) + K_{ic}\gamma_q + \omega_{VSG}x_f i_{cvd} \\ \dot{\gamma_d} &= i_{cvd}^* - i_{cvd} \\ \dot{\gamma_q} &= i_{cvq}^* - i_{cvq} \end{aligned}\right\} \quad (5)$$

$$\left.\begin{aligned} \frac{x_f}{\Omega_b}\frac{di_{cvd}}{dt} &= v_{cvd} - v_{od} - r_f i_{cvd} + \omega_{grid}x_f i_{cvq} \\ \frac{x_f}{\Omega_b}\frac{di_{cvq}}{dt} &= v_{cvq} - v_{oq} - r_f i_{cvq} - \omega_{grid}x_f i_{cvd} \\ \frac{b_f}{\Omega_b}\frac{dv_{od}}{dt} &= i_{cvd} - i_d + \omega_{grid}b_f v_{oq} \\ \frac{b_f}{\Omega_b}\frac{dv_{oq}}{dt} &= i_{cvq} - i_q - \omega_{grid}b_f v_{od} \end{aligned}\right\} \quad (6)$$

$$\left.\begin{aligned} \frac{x_g}{\Omega_b}\frac{di_d}{dt} &= v_{od} - V_g\cos(-\delta) - r_g i_d + \omega_{grid}x_g i_q \\ \frac{x_g}{\Omega_b}\frac{di_q}{dt} &= v_{oq} - V_g\sin(-\delta) - r_g i_q - \omega_{grid}x_g i_d \end{aligned}\right\} \quad (7)$$

$$\left.\begin{aligned} P &= i_d V_{od} + i_q V_{oq} \\ Q &= -i_q V_{od} + i_d V_{oq} \end{aligned}\right\} \quad (8)$$

III. STORAGE PLACEMENT

Although reference [14] points out that the virtual inertia can be provided by the DC link capacitor in the converter without further storage, this requires a large capacitor and is not suitable for providing the steady state droop power [14]. Thus, using ESS to emulate the inertia power and provide the droop power is a more comprehensive approach. The placement of the storage can be either on the DC side or the AC side of the grid side converter of the renewable system. The paper uses a wind turbine system as an example to illustrate these two structures.

A. DC Side/Inner ESS WTG

The ESS can be implemented into the DC port of the wind turbine generation (WTG) system. Reference [11-13]

introduce such an implementation based on the double-fed induction generation (type 3-WTG) and direct drive wind turbine (type 4-WTG) respectively. For example, Fig. 2 plots the VSG-controlled type 4-WTG [12,13].

In the original type 4-WTG system, the machine side converter (M-converter) has embedded variable frequency control strategy [10] with maximum power point tracking (MPPT) control. The grid side converter (G-converter) has a decoupled power control strategy [10] with a DC port voltage control to maintain the DC voltage, while feeding the generated wind power into the grid. The PLL is used to synchronize the G-converter to the grid. Under this control scheme, the type 4-WTG is a grid-feeder [9] which only injects the power into the grid and a grid-follower [9] to follow the grid frequency.

The implementation of the ESS in the DC port provides the possibility to control the DC port voltage through the ESS-tied converter (E-converter). Thus, the G-converter is free to move to the AC voltage control mode [12] with the VSG control to regulate the grid side voltage v_o and provide the virtual inertia. Under this control scheme, the total system behaves like a SG and the type 4-WTG becomes a grid-former to establish the voltage and frequency in the power system. The generated wind power P_M is fed forward to the swing equation P^* in (1), and the total system output P_{VSG} is the power P in (8) and (1). In this case the generated wind power in VSG is similar to the primary power in the SG, which also experiences a damping in power conversion caused by the emulated swing equation.

B. AC side/Outer ESS WTG

The inclusion of the ESS in the DC port of an existing wind turbine is obviously costly due to the modification of the converter capacity and its filter. An alternative is to implement the VSG control directly into the ESS and co-locate with the WTG as shown in Fig. 3. The WTG can be any type, and the generated power is injected into the grid directly. The VSG control in the ESS only regulates the ESS AC terminal voltage. From the grid point of view, the ESS is used only to support frequency and the total system is grid-feeding to feed the generated power and the compensated power. Although the virtual inertia can be provided by the ESS, the generated power from WTG does not contribute to the swing equation emulation and presents no damping on the power conversion.

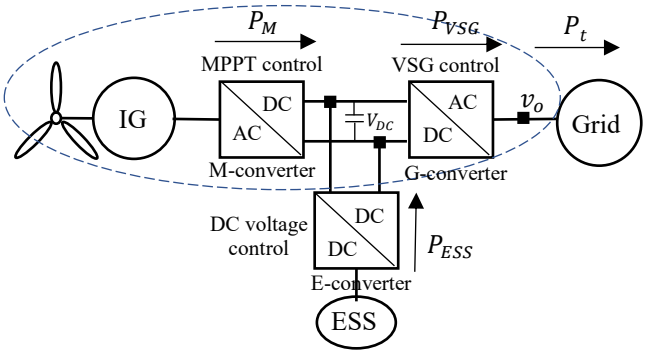

Fig. 2. Inner ESS WTG system

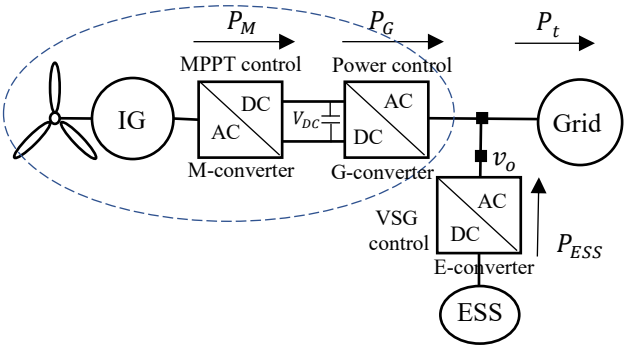

Fig. 3. Outer ESS WTG system

C. Simulation

The WTG system performance is first simulated in Matlab/Simulink using the full-switching model of the converter. The tested inner ESS and outer ESS WTG system are as shown in Fig. 2 and Fig. 3 respectively. The grid is set as a controllable frequency infinite bus and the M-converter is simplified as a controlled power source. Parameters and system settings are summarized in Table I. The total 1.5 MVA WTG system experiences the generated power increasing from 0 to 0.5 MW at 0.5 s and the grid frequency reducing from 50 Hz to 49.5 Hz with 10 Hz/s ramp at 1 s. Fig. 4 presents the result of the power injection to the grid.

TABLE I
HARDWARE VSG SETTINGS

Parameter	Value	Parameter	Value
PWM/Sampling time	1350/ 14.81e-6 s	Filter inductance	0.1 H
Rated Voltage $\widehat{v_g}$	8165 V	Filter resistance	0.12 Ω
Reference voltage V^*	8165 V	Filter capacitance	13 μF
Reference angular frequency ω^*	2π*50 Hz	Line inductance	0.1 H
VSG Inertia T_H	2.6 kW/(rad·s^{-2})	Line resistance	0.01 Ω
damping/droop K_D	169 kW/(rad·s^{-1})	Virtual inductance	0 H
reactive power droop K_v	0.0	Virtual resistance	15 Ω
Current controller P/I	222/326	Voltage controller P/I	0.008/ 1.87

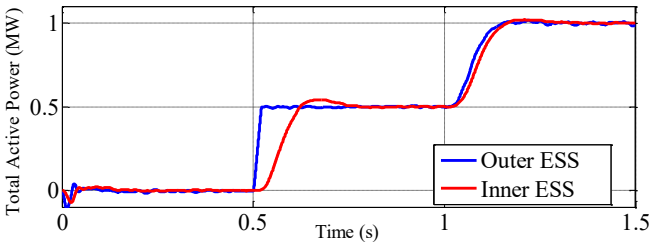

Fig. 4. Grid Power injection from WTG system

It can be seen in Fig. 4 that the inner ESS WTG system presents the inertia effect on both self-power generation and grid frequency variation, while the outer ESS WTG system has no inertia effect on the power generation. This is because the generated power in the former one goes through the swing equation then outputs from the VSG-controlled converter, while in the latter one, it directly outputs power from the decoupled power-controlled converter to the grid, which does not include the inertia. The mismatched power around 0.5 to 1

s in the inner ESS WTG system is absorbed by its ESS. On another hand, the frequency support from both WTG system is similar and its compensated power comes solely from the ESS.

IV. COMPARISON

The Matlab/Simulink test is open-loop i.e. based on feeding an infinite bus, where the injected power does not influence the grid frequency. This section will compare the inner ESS with outer ESS WTG system in the closed-loop. From the Matlab/Simulink open-loop result, these systems have the same response to the grid frequency variation while having a different response to the generated power change. Thus, the closed-loop analysis focuses on the effect of the generated power change on the system frequency where the system is modelled as a single equivalent SG with governor time constant T_{tg}, equivalent inertia M_{SG} and droop gain D_{SG}.

According to [15], the grid frequency to power transfer function can be reduced to the second order as (9).

$$G_{grid} = \frac{\Delta\omega_{grid}}{\Delta P} = \frac{T_{tg}s + 1}{T_{tg}M_{SG}s^2 + M_{SG}s + D_{SG}} \tag{9}$$

Rewriting (1) obtains the transfer function (10) of the power to the output voltage angle in VSG. According to [16], the angle to VSG real power output transfer function is related to the virtual impedance, line impedance and initial operating point E_0, δ_0 as (11). Where $r = r_v + r_g$, $x = x_v + x_g$. The block diagram for the simplified closed-loop VSG system (9~11) is plotted in Fig. 5.

$$G_s = \frac{\Delta\omega_{VSG}}{P^* - P} \cdot \frac{\Delta\delta}{\Delta\omega_{VSG}} = \frac{1}{Ms + D} \cdot \frac{1}{s} \tag{10}$$

$$H = \frac{\Delta P}{\Delta\delta} = \frac{3(E_0U_g r sin\delta_0 + E_0U_g x cos\delta_0)}{2(r^2 + x^2)} - \frac{3(E_0U_g r^2 r_v sin\delta_0 + E_0U_g x^2 r_v cos\delta_0)}{(r^2 + x^2)^2} \tag{11}$$

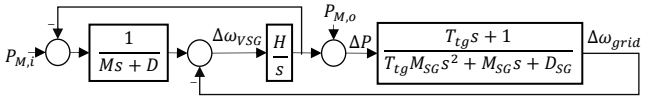

Fig. 5. VSG Closed-loop transfer function

In Fig. 5, as previously mentioned, the generated power in the inner ESS WTG system goes through the swing equation and is injected as $P_{M,i}$ ($P_{M,o} = 0$), while in the outer ESS the WTG system injects its power into the grid directly as $P_{M,o}$ ($P_{M,i} = 0$). The system performance is determined by the interaction of the VSG and SG. The VSG settings are identical to the ones used in the Matlab/Simulink model as given in Table I. The TG time constant T_{tg} is set to 1 s. We compare these two ESS WTG system performances in both high inertia and low inertia case.

A. High inertia

In the high inertia case, the system inertia and droop are mainly provided by the SG and TG respectively, i.e. $M_{SG} = 1000 * M$, $D_{SG} = 100 * D$. Fig. 6 presents the grid frequency variation after the generated wind power $P_{M,i}$ *and* $P_{M,o}$ for the inner and outer VSG respectively, step changes from 0 to 1 MW at 1 s.

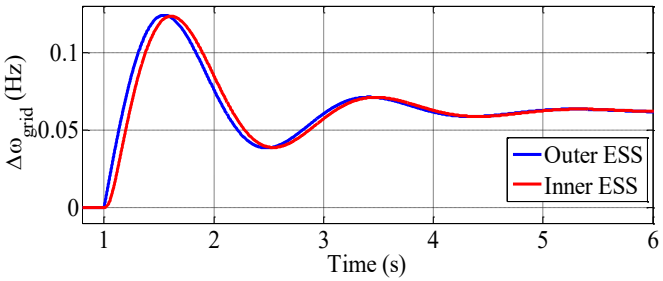

Fig. 6. frequency deviation in high inertia

From Fig. 6, the frequency deviation resulting from the inner and outer ESS WTG system generators are similar, because the high inertia system dynamics is dominated by the SG. The inner ESS result presents a slight delay compared to the outer ESS result, due to the virtual inertia and damping effects.

B. Low inertia

In the low inertia case, the system inertia and droop are mainly provided by the VSG-controlled WTG system, i.e. $M_{SG} = 0.1 * M$, $D_{SG} = D$. Fig. 7 presents the grid frequency variation after the generated wind power $P_{M,i}$ *and* $P_{M,o}$ for the inner and outer VSG respectively step changes from 0 to 10 kW at 1 s.

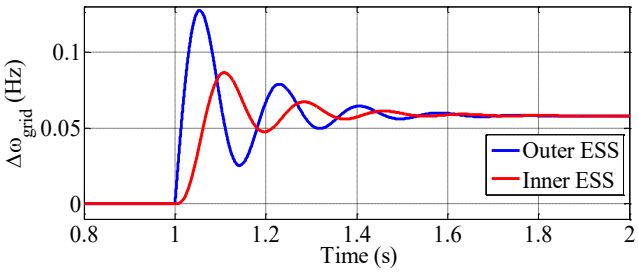

Fig. 7. frequency deviation in high inertia

In this case, the use of the inner ESS WTG in the system presents a better frequency response on the ROCOF and frequency nadir than the outer ESS WTG. This is because the generated power in the inner ESS WTG system first goes through the swing equation (10) with inertia and damping, while in case of the outer system the generated power goes first to the system and this experiencing the SG dynamics (9) first which consequently changes the frequency. The change in frequency then activates the VSG-controlled ESS response. Since the system inertia is dominated by the VSG, the inner ESS WTG system has better performance than the outer ESS WTG system on the system frequency dynamics.

V. CASE STUDY

The transfer function analysis is based on the simple two-bus system, while the real grid is meshed. This section aims to compare the outer and inner ESS WTG system using as a case study the stability of the IEEE 39-bus system (Fig. 8).

The work implements the VSG-controlled WTG system in the IEEE 39-bus system. The VSG-controlled WTG

system is modelled as shown in Fig. 2 or Fig. 3, where the inner ESS WTG system uses a direct drive wind turbine generator model detailed in [12], and the outer ESS WTG system uses a doubly fed induction generator (DIFG) model detailed in [17]. The VSG control model is given by (1~8). The ESS is assumed to work on the constant voltage with infinite capacity. To be a fair comparison, the WTG and VSG parameter in the outer and inner WTG system, as well as the system initial operating point, are set to be identical and given in Table II. G2 is the slack bus. The case study analyzes three scenarios. The first two scenarios consider a single VSG-controlled WTG system in the power system in order to compare the device response in the case of a contingency and in the case of variable to wind generation. The third scenario compares these two ESS placements in the power system with only WTG present, indicating the low inertia system.

To generate a contingency, at 1 s, Generator 10 is disconnected in the first scenario. The wind model applies a Weibull distribution wind speed formula [17]. The original 10-synchronous-generator power system data can be found in [17]. The simulation results in this section are obtained using Dome, a Python-based power system software tool [18].

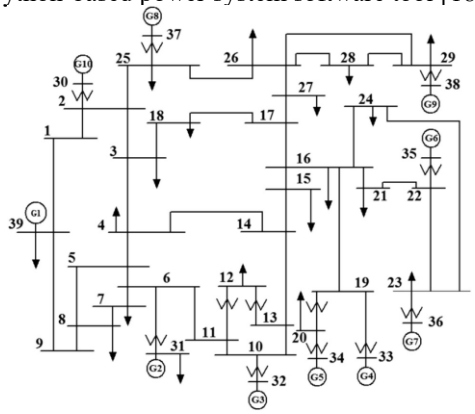

Fig. 8. New England 39-bus system

TABLE II
SCENARIO 1 SIMULATION PARAMETERS

Parameter	Value	Parameter	Value	Parameter	Value
S_{base}	100 MVA	V_n	220 kV	K_{pv}	25
M	20 s	x_f	0.08 pu	K_{iv}	5
D	400	r_f	0.01 pu	ω_f	20
K_v	0	b_f	0.34 pu	x_v	0.02 pu
K_{pc}	20	x_g	0.08 pu	r_v	0.01 pu
K_{ic}	10	r_g	0.005 pu		

A. *Scenario 1: One WTG with G10 lost*

In this scenario, a single VSG-controlled WTG replaces the SG (G5) at bus 34 (G5) and corresponds to an 8.29% wind penetration. The WTG in this scenario is considered to be working on a constant 13 m/s wind speed. At 1 s, as the contingency, G10 lost. Fig. 9 presents the grid frequency and the output active power from the WTG.

It can be seen from Fig. 9 (a) that the inclusion of the VSG control can improve the frequency response after the contingency. From Fig. 9 (a) and (b), as expected, the frequency support or active power compensation from WTG is not affected by the placement of the ESS. The compensated power is only from the ESS and determined by the VSG settings, i.e. virtual inertia and damping/droop gain.

B. *Scenario 2: wind generation in the hgih inertia system*

In this scenario, the tested system is same as in scenario 1. However, the WTG is working on the stochastic wind modelled as Weibull distribution wind speed, and the contingency is removed. Fig. 10 presents the grid frequency and the output active power from the WTG.

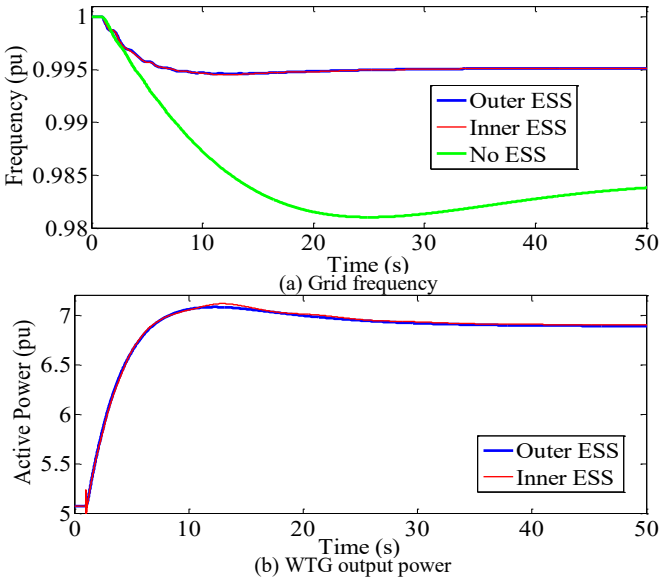

(a) Grid frequency
(b) WTG output power

Fig. 9. Scenario 1 results: one WTG with g10 lost

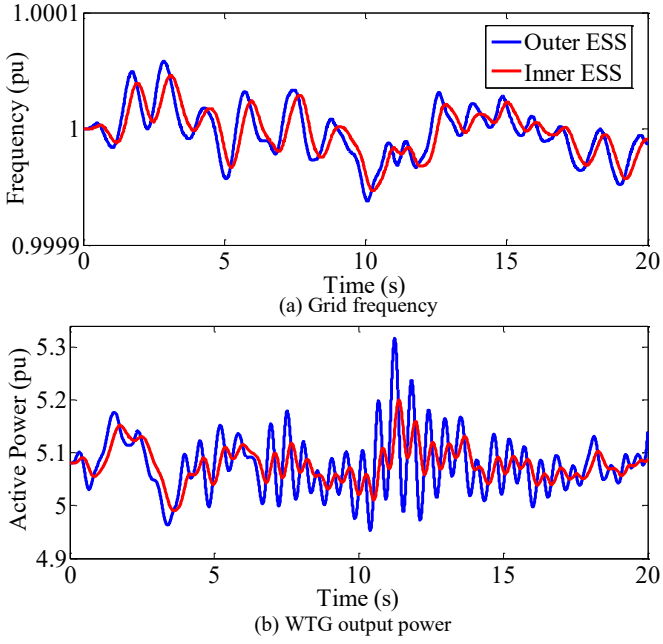

(a) Grid frequency
(b) WTG output power

Fig. 10. Scenario 2 results: wind generation in high inertia system

It can be seen in Fig. 10 (b) that the virtual inertia smooths the inner ESS active output, compared to the outer ESS WTG. However, because the system is dominated by the SG with high inertia, this difference barely has an influence on the grid

frequency (see Fig. 10 (a)). This verifies the transfer function analysis which indicated that the placement of the ESS is unimportant in the high inertia system.

C. Scenario 3: wind generation in the low inertia system

In this scenario, nine VSG-controlled WTGs replace the SGs (G1 and G3~10) and correspond to 91.66% wind penetration. The WTGs in this scenario are considered to work on stochastic wind modelled as Weibull distribution wind speed. The wind speed dynamics for each WTG is different. Fig. 11 presents the grid frequency and the output active power from the WTG.

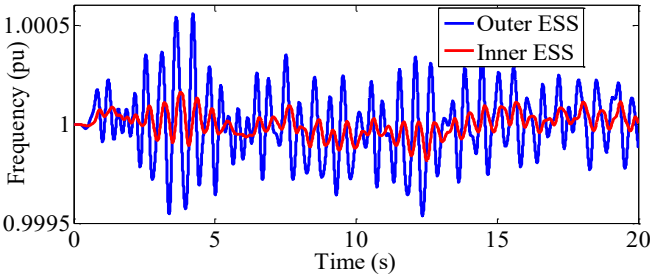

Fig. 11. Scenario 3 results: wind generation in low inertia system

It can be seen from Fig. 11 that the inner ESS WTG can significantly improve the system frequency dynamics caused by the wind power generation. Note the behavior of each WTG is similar to that shown in Fig. 10 (b). However, in this scenario, there are nine WTGs, and the system inertia is dominated by the WTG. The effect of the damped generation is amplified. It verifies that in low inertia systems, the inner ESS WTG has more benefit for the grid frequency regulation than the outer ESS WTG.

VI. Conclusion

The paper analyzes the effects of the placement of the VSG controlled ESS in the WTG on the system stability. From the simulation in IEEE 39-bus system in Dome, we could draw the following conclusions:

1) From the support point of view, the placement of the ESS does not affect the system transient stability. In transient, under the VSG control, the virtual inertia power and droop power is provided by the ESS regardless of the wind turbine.

2) From the generation point of view, inner ESS WTG is more advanced than outer ESS WTG. In the SG dominated system or high inertia system, although the inner ESS WTG can help smooth its generation, it does not have an apparent influence on the system stability. Thus, the ESS can be implemented in either inner or outer configuration. However, if the system is dominated by the power electronics generation, the inner ESS WTG has a significant benefit on the system frequency variation.

Of course, even using outer ESS structure, an improved coordinated control could be designed to regulate the ESS to absorb the variable power from the wind generation and thus make the outer ESS WTG behave more like the inner ESS WTG. This kind of control will be researched in the future.

References

[1] H. Beck and R. Hesse, "Virtual Synchronous Machine," 2007 9th International Conference on Electrical Power Quality and Utilisation, pp.1-9, 2007.

[2] K. Sakimoto, Y. Miura, and T. Ise, "Stabilization of a Power System with a Distributed Generator by a Virtual Synchronous Generator Function", 2011 IEEE 8th International Conference on Power Electronics and ECCE Asia (ICPE & ECCE), pp. 1498 - 1505,2011.

[3] Q.-C. Zhong and G. Weiss, "Synchronverter: Inverters that mimic synchronous generators," IEEE Trans. In. Electron., vol. 58, no. 4, pp. 1259-1267, Apr. 2011.

[4] Q.-C. Zhong, P.-L. Nguyen, Z. Ma, and W. Sheng, "Self-synchronized synchronverters: Inverters without a dedicated synchronization unit," IEEE Trans. Power Electron., vol. 29, no. 2, pp. 617-630, Feb. 2014.

[5] S. Arco, J. A. Suul and O. B. Fosso, "A Virtual Synchronous Machine implementation for distributed control of power converters in Smart Grids," Electric Power Systems Research, Vol. 122, pp. 180-197, May 2015.

[6] S. Acro, J. A. Suul and O. B. Fosso, "Small-signal modelling and parametric sensitivity of a Virtual Synchronous Machine", 2014 Power Systems Computation Conference (PSCC), Wroclaw, Poland, 18-22 Aug. 2014.

[7] S. Acro, J. A. Suul and O. B. Fosso, "Control system tuning and stability analysis of Virtual Synchronous Machines", 2013 Energy Conversion Congress and Exposition (ECCE), Denver, CO, USA, 15-19 Sept. 2013.

[8] J. Chen, M. Liu, C. O'Loughlin, F. Milano and T. O'Donnell, "Modelling, Simulation and Hardware-in-the-Loop Validation of Virtual Synchronous Generator Control in Low Inertia Power System," *2018 Power Systems Computation Conference (PSCC)*, Dublin, 2018, pp. 1-7.

[9] J. Rocabert, A. Luna, F. Blaabjerg and P. Rodriguez, "Control of Power Converters in AC Microgrids," IEEE Trans. Power Electronics, vol. 27, no. 11, Nov. 2012.

[10] A. Yazdani and R. Iravani, "Voltage-soured Converters in Power Systems," WILEY IEEE PRESS, March 2010, ISBN: 978-0-470-52156-4.pp204-269.

[11] S. Wang, J. Hu, X. Yuan and L. Sun, "On Inertial Dynamics of Virtual-Synchronous-Controlled DFIG-Based Wind Turbines," in *IEEE Transactions on Energy Conversion*, vol. 30, no. 4, pp. 1691-1702, Dec. 2015.

[12] Y. Ma, W. Cao, L. Yang, F. (. Wang and L. M. Tolbert, "Virtual Synchronous Generator Control of Full Converter Wind Turbines With Short-Term Energy Storage," in *IEEE Transactions on Industrial Electronics*, vol. 64, no. 11, pp. 8821-8831, Nov. 2017.

[13] J. Chen, M. Liu and T. O'Donnell, "Replacement of Synchronous Generator by Virtual Synchronous Generator in the Conventional Power System," IEEE PES General Meeting, Atlanta, GA, 4-8 August 2019.

[14] C. Li, Y. Li, Y. Cao, H. Zhu, C. Rehtanz and U. Häger, "Virtual Synchronous Generator Control for Damping DC-Side Resonance of VSC-MTDC System," in *IEEE Journal of Emerging and Selected Topics in Power Electronics*, vol. 6, no. 3, pp. 1054-1064, Sept. 2018.

[15] Y. Hirase, K. Sugimoto, K. Sakimoto and T. Ise, "Analysis of Resonance in Microgrids and Effects of System Frequency Stabilization Using a Virtual Synchronous Generator," in *IEEE Journal of Emerging and Selected Topics in Power Electronics*, vol. 4, no. 4, pp. 1287-1298, Dec. 2016.

[16] J. Chen and T. O'Donnell, "Parameter Constraints for Virtual Synchronous Generator Considering Stability," in *IEEE Transactions on Power Systems*, 2019 (Early Access).

[17] F. Milano, "Power System Modelling and Scripting", Springer, London, August 2010.

[18] F. Milano, "A Python-based Software Tool for Power System Analysis," IEEE PES General Meeting, Vancouver, Canada, 21-25 July 2013.